Progress In Electromagnetics Research, Vol. 126, 539–553, 2012

A NEW PLASMA ANTENNA OF BEAM-FORMING

X. P. Wu[1,2,*], J. M. Shi[1,2], Z. S. Chen[1], and B. Xu[2]

[1]State Key Laboratory of Pulsed Power Laser Technology, Hefei, Anhui, China

[2]Key Laboratory of Infrared and Low Temperature Plasma of Anhui Province, Hefei, Anhui, China

Abstract—In this paper, a new plasma antenna of beam-forming is investigated based upon the interaction of plasma elements due to the incident electromagnetic wave. It presents a study of the multiple scattering from argon plasma cylinders rigorously applying boundary value method, grounded on the properties of electromagnetic wave transmitted in the argon plasma. Approximate expressions for the total radiation of plasma antenna in the far field are derived briefly. Such a novel plasma antenna of beam-forming, according to the research, exhibits interesting performance in terms of radiation efficiency, beam-forming and beam-scanning. Valid results are brought forth to demonstrate the capabilities of such antenna of two scales. Comparisons are given in detail as well.

1. INTRODUCTION

The concept of using plasma as the effective reflector in radio frequency antenna is not new. For the past decades, numerous contributions have been done continuously on the plasma antennas in various realms of application, such as communication [1–10], radio detection [11], target directing [12] and so on [13]. In the area of communication, the plasma element was considered as an effective radiator to release the electromagnetic energy just as the metal element did. Several techniques for producing the plasma were also introduced and verified practicality. While, in the fields of radio detection and target directing, the plasma element was treated as a reflector in the planar shape to reflect the well configured electromagnetic wave. Antenna beam or multi-beams were produced in expected directions according to the

Received 19 February 2012, Accepted 27 March 2012, Scheduled 4 April 2012

* Corresponding author: Xiao Po Wu (wuxiaopo2337@163.com).

authors Mathew [11] and Cheng [12]. In this regard, the analysis of beam-forming and beam-scanning will be also outlined in this paper to predict the perfect performance of such a novel plasma antenna. To be different from the reflector of planar shape in the case of [11, 12], the plasma elements used in this paper take the form of cylindrical geometry to scatter the wave energy and then concentrate it in predicted direction. On the other hand, the plasma elements in this paper could be energized in more flexible way (e.g., high-frequency AC discharging in vacuum tubes) rather than the ignition in a big heavy cylinder which takes much space.

It is precisely an original idea for the antenna operating in multi-beams or beam-scanning, although many investigators [14–25] have been working on the techniques for several years. The plasma antenna of beam-forming examined in this paper is composed of plasma elements as reflector (or scatterer to be more accurate) and additional omnidirectional radiation source. In essence, the mechanism of the beam-forming is based upon the switchable state of plasma elements (i.e., plasma energized or de-energized) as well as the interaction between the plasma elements [26, 27] and the incident electromagnetic wave. Multiple scattering [28–33] by the plasma cylinders is investigated rigorously applying boundary value method [34] due to the continuity of electromagnetic tangential components on the boundary. In all subsequent analysis, we assume that the radiation source is working at frequencies well below the eigenfrequency of plasma energized so as to prevent the electromagnetic energy from leaking by penetrating the plasma shield. Ample numerical results are figured out followed by elaborate explanations and comparisons. It is shown that such kind of plasma antenna exhibits excellent performances in the aspects of beam-forming, beam-scanning, etc.

2. FORMULATION

Consider N parallel homogeneous argon plasma cylinders as shown in Figure 1. These plasma cylinders of the same radii R are situated such that their axes are parallel to the z-axis of the cylindrical coordinate system used. The centre of the ith plasma cylinder denoted by (d, ψ_i) is located equidistantly with respect to the origin, where placed an omnidirectional antenna responsible for the electromagnetic energy radiation.

The electromagnetic field satisfying the Maxwell equation could

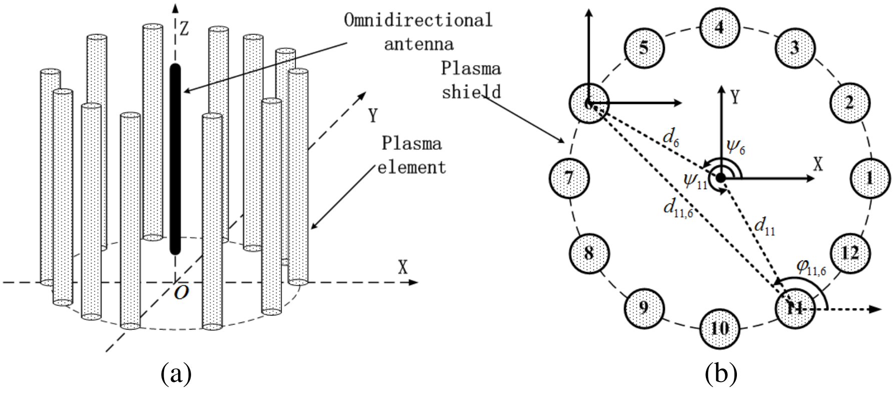

Figure 1. Geometry of the plasma antenna of beam-forming (12 plasma elements in this case). (a) The solid side view of the antenna. (b) The top plan view of the antenna.

be specified as follows

$$\begin{cases} \nabla \times \vec{E} = -j\omega\vec{B} \\ \nabla \times \vec{B} = j\frac{\omega}{c^2}\varepsilon_{ri}\vec{E} \end{cases} \tag{1}$$

where $c = 1/\sqrt{\mu_0\varepsilon_0}$ is the speed of light in free space, μ_0 the space permeability, ε_0 the space permittivity, and ε_{ri} the complex relative permittivity of ith plasma cylinder, given by

$$\varepsilon_{ri} = 1 - \frac{\omega_{pe,i}^2}{\omega(\omega - jv_i)} \quad i = 1, 2, \ldots, N \tag{2}$$

Meanwhile, the conductivity of ith plasma cylinder is obtained as

$$\sigma_i = \frac{\varepsilon_0\omega_{pe,i}^2}{j\omega + v_i} \tag{3}$$

where $\omega_{pe,i}$ is the angular frequency of plasma given by $\omega_{pe,i} = \sqrt{\frac{n_{ei}e^2}{\varepsilon_0 m_e}}$, n_{ei} the electron density of ith plasma cylinder, m_e the electron mass, e the charge of the electron, ν_i the collision frequency of ith plasma cylinder, and ω the angular frequency of incident wave.

The propagation of the incident wave in the plasma could be characterized in another term by the complex refractive index as follows

$$\tilde{n} = \sqrt{\varepsilon_r} = \sqrt{1 - \frac{\omega_{pe}^2}{\omega(\omega - jv)}} = n - j\chi \tag{4}$$

where n, χ represent the refraction and attenuation indices of the plasmas, respectively. One can easily write down their specific forms as follows

$$\begin{cases} n = \sqrt{\frac{1}{2}\left(1 - \frac{\omega_{pe}^2}{\omega^2+v^2}\right) + \frac{1}{2}\sqrt{\left(1 - \frac{\omega_{pe}^2}{\omega^2+v^2}\right)^2 + \left(\frac{\omega_{pe}^2}{\omega^2+v^2} \cdot \frac{v}{\omega}\right)^2}} \\ \chi = \sqrt{-\frac{1}{2}\left(1 - \frac{\omega_{pe}^2}{\omega^2+v^2}\right) + \frac{1}{2}\sqrt{\left(1 - \frac{\omega_{pe}^2}{\omega^2+v^2}\right)^2 + \left(\frac{\omega_{pe}^2}{\omega^2+v^2} \cdot \frac{v}{\omega}\right)^2}} \end{cases} \tag{5}$$

In this analysis, we assume that the original wire source is carrying a current I aligned with the z-axis. As such, the electric field has a z component only with all vectors independent of z to be

$$E_z = -\frac{j\omega\mu_0 I}{2\pi} K_0(jk_0\rho) e^{-jk_0 \vec{e}_n \cdot \vec{\rho}} \tag{6}$$

where $k = 2\pi/\lambda$ is the wave number, $\vec{e}_n = \vec{e}_x \cos\alpha + \vec{e}_y \cos\beta + \vec{e}_z \cos\gamma$ refers to the direction of outgoing wave, $\vec{\rho} = \vec{e}_x x + \vec{e}_y y + \vec{e}_z z$ represents the observation point. As a result, the expanded incident wave relative to the ith plasma cylinder may be expressed as

$$E_{zi}^{inc} = E_0 \sum_{n=-\infty}^{\infty} j^{-n} J_n(k_0\rho_i) e^{jn(\varphi_i - \psi_i)} \tag{7}$$

where

$$E_0 = -\frac{j\omega\mu_0 I}{2\pi} K_0(jk_0 d) e^{-jk_0 d} \tag{8}$$

$$\psi_i = \frac{2\pi}{N}(i-1) \tag{9}$$

and $J_n(x)$, $K_0(x)$ are the Bessel function of the first kind and Bessel function of the second modified kind, respectively, both with the order n (in this case $n = 0$ for the second modified kind) and argument x.

The corresponding scattered field from the ith plasma cylinder is given by

$$E_{zi}^{s} = E_0 \sum_{n=-\infty}^{\infty} A_{ni} H_n^{(2)}(k_0\rho_i) e^{jn\varphi_i} \tag{10}$$

and the transmitted field component inside the ith plasma is

$$E_{zi}^{t} = E_0 \sum_{n=-\infty}^{\infty} B_{ni} J_n(k_i\rho_i) e^{jn\varphi_i} \tag{11}$$

where k_0, k_i are the wave numbers of free space and plasma, respectively. A_{ni} and B_{ni} are the unknown coefficients related to

ith plasma cylinder, which includes the multiple interactions. The superscripts s and t refer to the scattered fields in free space and the fields transmitted in the plasma, respectively, while the subscripts z denotes the z component. $H_n^{(2)}(x)$ is the Hankel function of second kind with the order n and argument x.

On the surface of the plasma cylinders, the boundary conditions are written as below

$$\begin{cases} E_{z1}^{inc} + \sum\limits_{l=1}^{12} E_{zl}^{s} = E_{z1}^{t}\Big|_{\rho_1=R}, \quad H_{\varphi 1}^{inc} + \sum\limits_{l=1}^{12} H_{\varphi l}^{s} = H_{\varphi 1}^{t}\Big|_{\rho_1=R} \\ E_{z2}^{inc} + \sum\limits_{l=1}^{12} E_{zl}^{s} = E_{z2}^{t}\Big|_{\rho_2=R}, \quad H_{\varphi 2}^{inc} + \sum\limits_{l=1}^{12} H_{\varphi l}^{s} = H_{\varphi 2}^{t}\Big|_{\rho_2=R} \\ \cdots\cdots \\ \cdots\cdots \\ \cdots\cdots \\ E_{z12}^{inc} + \sum\limits_{l=1}^{12} E_{zl}^{s} = E_{z12}^{t}\Big|_{\rho_{12}=R}, \quad H_{\varphi 12}^{inc} + \sum\limits_{l=1}^{12} H_{\varphi l}^{s} = H_{\varphi 12}^{t}\Big|_{\rho_{12}=R} \end{cases} \tag{12}$$

where, the tangential components of the magnetic field H_φ can be derived by substituting (10) and (11) into (1), which yields

$$H_{\varphi i}^{s} = \frac{1}{jk_0\eta_0}\frac{\partial E_{zi}^{s}}{\partial \rho_i} \tag{13}$$

$$H_{\varphi i}^{t} = \frac{1}{jk_i\eta_i}\frac{\partial E_{zi}^{t}}{\partial \rho_i} \tag{14}$$

where η_0, η_i are the wave impedances for the free space and ith plasma, respectively.

To be more detailed, the continuity of the electromagnetic components on the boundary necessitates a transfer of the field from the remaining sub-coordinates to the local sub-coordinate, in other words, one has to use the addition theorem [35] for the Hankel functions to express the electric field components E_{zl}^{s} $(l = 1, 2, \ldots, N, l \neq i)$ in terms of E_{zi}^{s} (it is the same with magnetic field components), and vice versa. The transformation from the qth sub-coordinate to the pth sub-coordinate could be written as

$$H_n^{(2)}(k\rho_q)e^{jn\varphi_q} = \sum_{m=-\infty}^{+\infty} J_m(k\rho_p)H_{m-n}^{(2)}(kd_{pq})e^{jm\varphi_p}e^{-j(m-n)\varphi_{pq}} \tag{15}$$

where

$$d_{pq} = \sqrt{d_p^2 + d_q^2 - 2d_pd_q\cos(\psi_p - \psi_q)} \tag{16}$$

$$\varphi_{pq} = \begin{cases} \arccos\left(\frac{d_q \cos\psi_q - d_p \cos\psi_p}{d_{pq}}\right), & d_q \sin(\psi_q) \geq d_p \sin\psi_p \\ -\arccos\left(\frac{d_q \cos\psi_q - d_p \cos\psi_p}{d_{pq}}\right), & d_q \sin(\psi_q) < d_p \sin\psi_p \end{cases} \tag{17}$$

From the above expressions, one notices that the infinite series will result in infinite equations to make the calculation impossible. Therefore, a reasonable truncation should be adopted and actually we always do like this. The cut-off integer is practically related to the radius and type of the ith plasma cylinder by the relation $n_0 \approx 3k_iR$. Thus all the unknown coefficients A_{ni}, B_{ni} $(i = 1, 2, \ldots, N, n = -n_0, -n_0+1, \ldots, n_0-1, n_0)$ can be derived from $2(2n_0+1)N$ equations, half of which concerning with A_{ni} could be cast into a matrix form as

$$[C] = [S][A] \tag{18}$$

where, the elements of matrix $[C]$ are

$$c_i^m = e^{-jk_0d} j^{-m} e^{-jm\psi_i}, \quad i = 1, 2, \ldots, N \tag{19}$$

and the elements of coefficients matrix $[S]$ are

$$s_{il}^{mn} = \begin{cases} -H_{m-n}^{(2)}(k_0d_{il})e^{-j(m-n)\varphi_{il}} & i \neq l \\ \frac{\eta_i H_m^{(2)'}(k_0R)J_m(k_iR) - \eta_0 H_m^{(2)}(k_0R)J_m'(k_iR)}{\eta_0 J_m(k_0R)J_m'(k_iR) - \eta_i J_m'(k_0R)J_m(k_iR)} & i = l \,\&\, n = m \\ 0 & i = l \,\&\, n \neq m \end{cases} \tag{20}$$

Once the scattering coefficients are obtained, the coefficients B_{ni} can be readily evaluated.

Then the total scattered electric field is given by

$$E_{tot}^s = \sum_{i=1}^{N} \sum_{n=-n_0}^{n_0} A_{ni} H_n^{(2)}(k_0\rho_i) e^{jn\varphi_i} \tag{21}$$

In the far field, where $k_0\rho_i \gg 1$, we employ the approximations

$$\begin{cases} \varphi_1 \approx \varphi_2 \approx \ldots \approx \varphi_i \approx \varphi \\ \rho_i \approx \rho - d\cos(\varphi - \psi_i) \end{cases} \tag{22}$$

Together with the asymptotic value of the Hankel function for the large argument, i.e.,

$$H_n^{(2)}(k_0\rho_i) = \sqrt{\frac{2}{\pi k_0 \rho}} e^{-jk_0\rho + jk_0 d\cos\varphi + j\frac{2n+1}{4}\pi} \tag{23}$$

As a result, (21) evolves into

$$E_{tot}^s = \sqrt{\frac{2}{\pi k_0 \rho}} e^{-jk_0\rho} e^{j\frac{\pi}{4}} \sum_{i=1}^{N} \sum_{n=-n_0}^{n_0} A_{ni} j^n e^{jk_0 d\cos(\varphi-\psi_i)} e^{jn\varphi} \tag{24}$$

from which one can settle the total field distribution in the far filed as a sum of the total scattered field plus the incident field from the source. It is

$$E_{tot} = E_{inc} + E_{tot}^s \tag{25}$$

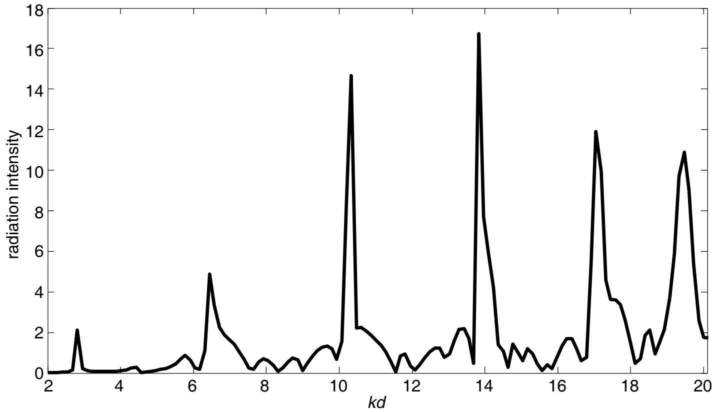

Figure 2. Radiation intensity versus kd for antenna of 12 plasma elements.

3. NUMERICAL RESULTS AND DISCUSSION

For the sake of convenience and maneuverability of experiment, we assume that the Argon plasma columns are formed in the T12 (or T8) discharging tube with noble pressure 1 to 5 torr and the length of the plasma tubes are irrelevant to the analysis [36, 37]. Moreover, fluctuations of plasma density arising from occasional striation discharge can be ignored. As a result, the problem becomes two dimensional and permits an exact solution.

Figure 2 portrays the radiation power for the antenna of Figure 1. In this case, the homemade plasma elements are energized via the equal rectifiers under the circumstance of room temperature, and the electron densities and collision frequencies are averaged by $n_e = 9.24 \times 10^{17}\,\mathrm{m}^{-3}$, $\bar{v}_e = 6.83 \times 10^7\,\mathrm{Hz}$ respectively. The distance between plasma shield and the origin is set to $d = 0.0641\,\mathrm{m}$. Before the plasma antenna works, the plasma elements are all energized so as to make the electromagnetic energy from the omnidirectional antenna surrounded by plasma shield without leaking. The results are derived by leaving one of the plasma elements (i.e., the No. 1 plasma cylinder) de-energized to free the electromagnetic energy along the azimuth angle $\varphi = 0$. As we can see, the leaking radiation power varies periodically with the electrical distance due to the interactions between the plasma elements. Leaps occur when interactions coherently oscillate to the optimum.

Figure 3 is the schematic representation of radiation lobes produced by the antenna of Figure 1. In Figure 3(a), the polar graphs illustrate the single beams for the cases of $f = 4.3\,\mathrm{GHz}$, $5.9\,\mathrm{GHz}$

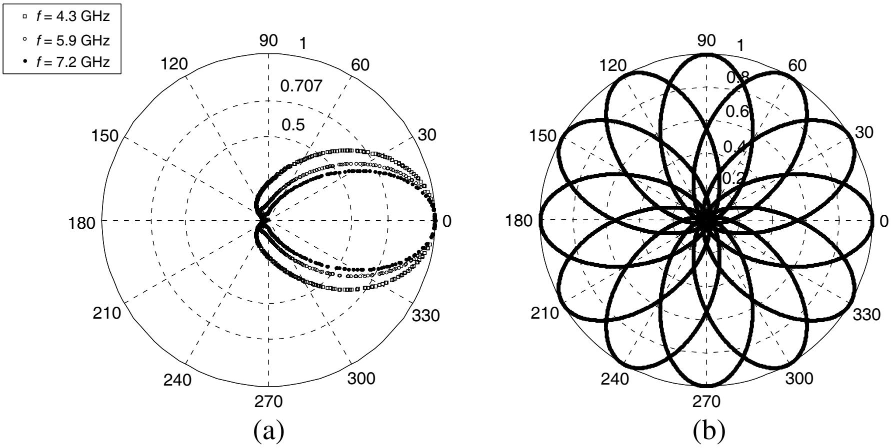

Figure 3. Radiation pattern for the plasma antenna. (a) Single beam at 4.3 GHz, 5.9 GHz and 7.2 GHz. (b) Single beam-scanning at 8.1 GHz.

and 7.2 GHz respectively. The radiation intensity in the far field in each case is normalized, from which one could readily find that the lobe becomes more focused as the frequency increases. The plots are obtained by leaving the first plasma cylinder de-energized in the same way. When it occurs to another plasma element, an emerging single beam is formed along the corresponding azimuth angle with the former lobe fading away in microseconds. By doing so in sequence, scanning of single beam will commence with the step of thirty degrees as Figure 3(b) demonstrates for the higher frequency $f = 8.1$ GHz. To be theoretically, one could make the lobe aiming at any direction if the surrounding shield is composed of sufficient plasma elements. Interesting enough, these behaviors of beam forming and scanning cannot be completed by the traditional metal element except for the plasma element. The reason accounting for this may be that the electromagnetic wave will be transmitted just as in the free space when the plasma cylinder is destroyed. No scattering and no interaction subsequently happen to this de-energized plasma cylinder.

Figure 4 is schematic diagrams of two beams for the antenna of Figure 1 working at $f = 8.1$ GHz. The lobes are produced by leaving arbitrary two non-adjacent plasma elements shut off, Figure 4(a) for the cylinders 1th & 8th off and Figure 4(b) for the cylinders 3th & 10th off. In contrast to the case of single beam, this kind of beam-forming mechanism leads to a multiway communication at the costs of lower radiation efficiency and possible lobe distortion. Less plasma elements involved in the scattering and interaction are necessarily responsible for the lower radiation efficiency, while the possible lobe distortion may arise from the uncontrollable intervene and unexpected diffraction of the apertures due to the destroyed plasma cylinders. Serious distortion

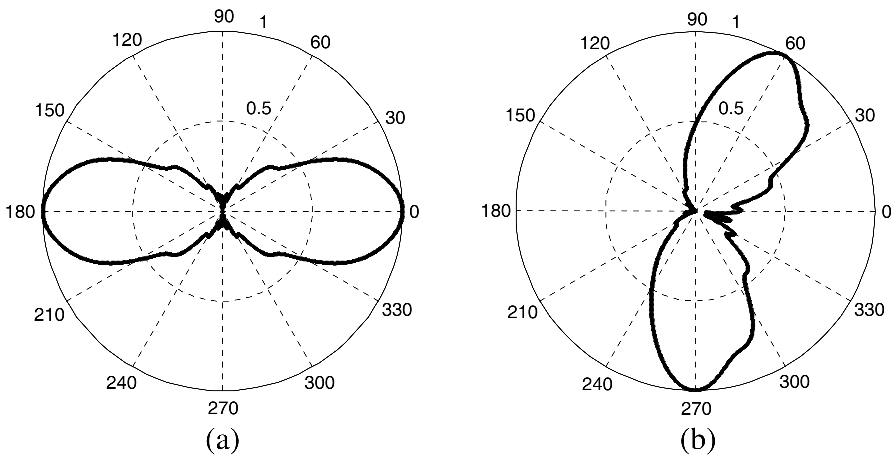

Figure 4. Double beams for the antenna at 8.1 GHz. (a) Plasma of 1th and 7th de-energized. (b) Plasma of 3th and 10th de-energized.

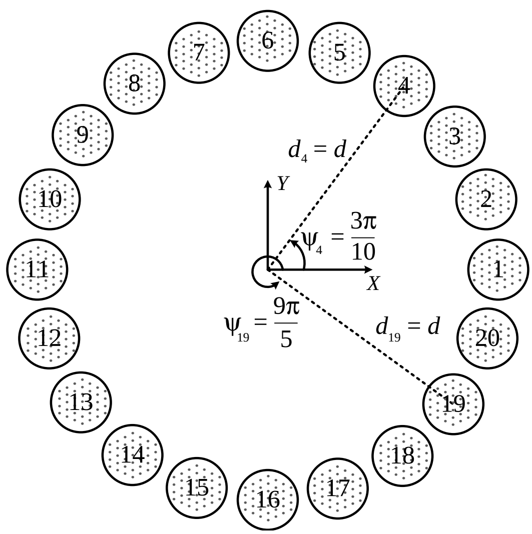

Figure 5. The top plan view of the plasma antenna of beam-forming (20 plasma elements involved).

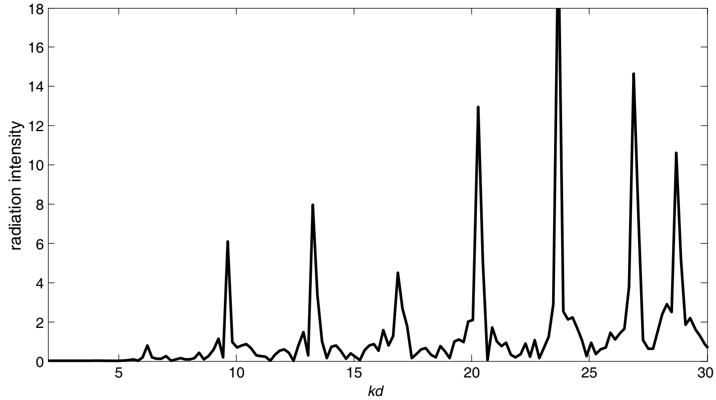

Figure 6. Radiation intensity versus kd for antenna of 20 plasma elements.

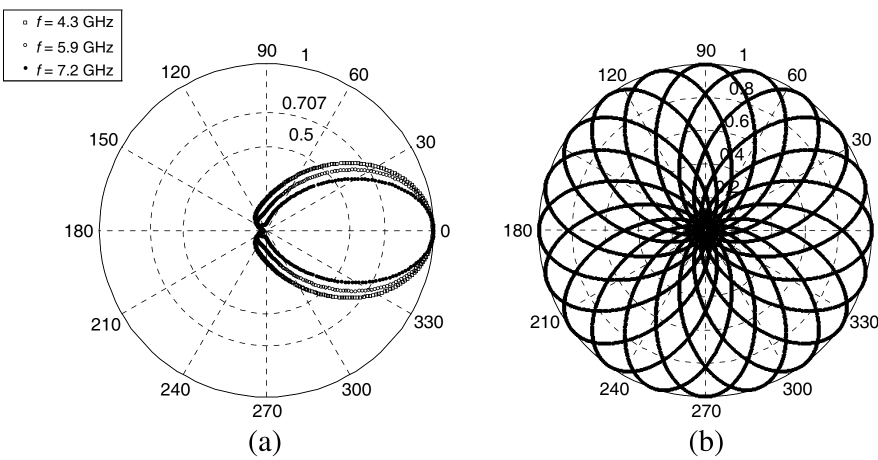

Figure 7. Radiation pattern for the plasma antenna of 20 plasma elements. (a) Single beam at 4.3 GHz, 5.9 GHz and 7.2 GHz. (b) Single beam-scanning at 8.1 GHz.

will emerge for the closer distance between the two apertures.

For the further investigation of such kind of plasma antenna, in this paper, a larger scale of shield consisting twenty identical plasma elements are examined as well (see Figure 5). The omnidirectional antenna mentioned above is once again employed and the distance between the origin and the shield increases to $d = 0.0958\,\text{m}$. Figures 6

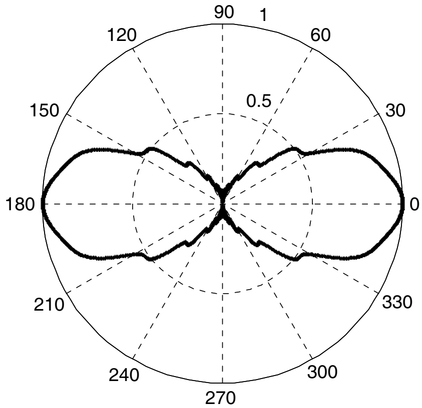

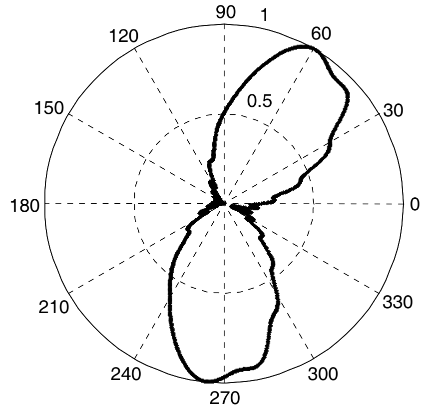

Figure 8. Double beams for the antenna at 8.1 GHz. (a) Plasma of 1th and 11th de-energized. (b) Plasma of 4th and 16th de-energized.

to 8 are presented in comparisons with the corresponding cases of plasma antenna of Figure 1. From these comparisons, one could draw the conclusions that the antennas of two scales have practically the comparative single beam half width at the same frequency due to the basically equal-sized apertures. Fortunately enough, the larger one is characterized by better azimuth resolution and directivity, which means greater orientation and longer communication distance. In addition, relatively intense intervenes and diffractions resulting from more plasma elements involved in the scattering and interaction may bring about the worse multi-beam forming. However, there are two points that merit emphasis. The first point is that the antenna of larger scale does not always behave badly in the multi-beam forming. It just depends. The conclusion is only for the given frequency $f = 8.1\,\text{GHz}$ and equal-sized plasma elements used in both antennas. The second point is that the antenna comprising less plasma elements, other than the larger-scale one even for its better performance, is preferably applied in the wireless communication of local area for its short distance of transmissions and smart structure. After all, communications in limited area, especially in offices, sometimes mean security with no interception by unauthorized recipient not far away.

4. CONCLUSION

A rigorous and complete model for a new plasma antenna of beam-forming has been presented. Mathematical calculations are performed to predict the radiation pattern of plasma antenna. Valid results indicate that such a plasma antenna shows good performance in the aspects of beam-forming, beam-scanning and radiation efficiency. To be an intact research, however, further concrete works have to be done in the future. They are the influence brought by the plasma density, plasma collision, radii and separations of the plasma elements.

ACKNOWLEDGMENT

The authors wish to acknowledge the financial assistance of the National Defense Pre-Research Foundation of China (Grant No. 9140A31030310JB39) and Key Laboratory of Infrared & Low Temperature Plasma Fund of Anhui Province (Grant No. 2007A0103013Y) as well as the faculty of State Key Laboratory of Pulsed Power Laser Technology who made this research possible.

REFERENCES

1. Dwyer, T. J., J. R. Greig, D. P. Murphy, J. M. Perina, and R. E. Pechacek, "On the feasibility of using an atmospheric discharge plasma as an RF antenna," *IEEE Trans. Antennas Propag.*, Vol. 32, 141–146, 1984.
2. Brog, G. G., J. H. Harris, D. G. Miljak, and N. M. Martin, "Application of plasma columns to radiofrequency antennas," *Appl. Phys. Lett.*, Vol. 74, 3272–3274, 1999.
3. Brog, G. G., J. H. Harris, N. M. Martin, D. Thorncraft, R. Milliken, et al., "Plasma as antenna: Theory, experiment and applications," *Phys. Plasma.*, Vol. 7, 2198–2202, 2000.
4. Rayner, J. P., A. P. Whichello, and A. D. Cheetham, "Physical characteristics of a plasma antenna," *Proc. 11th Int. Conf. Plasma Physics*, 392–395, Sydney, Australia, Jul. 2002.
5. Fathy, A. E., A. Rosen, H. S. Owen, and F. Mc-Ginty, "Silicon-based reconfigurable antennas — Concepts, analysis, implementation and feasibility," *IEEE Trans. Microwave Theory Tech.*, Vol. 51, 1650–1661, 2003.
6. Rayner. J. P. and A. P. Whichello, "Physical characteristics of plasma antennas," *IEEE Trans. Plasma. Sci.*, Vol. 32, 269–281, 2004.

7. Alexeff, I. and T. Anderson, "Experimental and theoretical results with plasma antennas," *IEEE Trans. Plasma. Sci.*, Vol. 34, No. 2, Apr. 2006.
8. Alexeff, I., T. Anderson, E. Farshi, N. Karnam, and N. R. Pulasani, "Recent results for plasma antennas," *Phys. Plasma.*, Vol. 15, 057104, 2008.
9. Russo. P., G. Cerri, and E. Vecchioni, "Self-consistent model for the characterization of plasma ignition by propagation of an electromagnetic wave to be used for plasma antennas design," *IET Microwave Antennas Propag.*, Vol. 4, 2256–2264, 2010.
10. Kumar, R. and D. Bora, "A reconfigurable plasma antenna," *J. Appl. Phys.*, Vol. 107, 053303, 2010.
11. Mathew, J., R. A. Meger, R. F. Fernsler, D. P. Murphy, R. E. Pechacek, and W. M. Manheimer, "Electronically steerable plasma mirror based radar antenna," *10th International Conference on Antenna and Propagation*, No. 436, 1469–1473, Apr. 14–17, 1997.
12. Cheng, Z. F., "Design and research on plasma microwave reflector," Center for Space Science and Applied Research, China, Beijing, 2010.
13. Haleakala Research and Development, Inc., *Commercial Smart Plasma Antenna Prototype*, Brookfield, Massachusetts, USA, 2008.
14. Kamarudin, M. R. B., P. S. Hall, F. Colombel, and M. Himdi, "Electronically switched beam disk-loaded monopole array antenna," *Progress In Electromagnetics Research*, Vol. 101, 339–347, 2010.
15. Liu, J., W.-Y. Yin, and S. He, "A new defected ground structure and its application for miniaturized switchable antenna," *Progress In Electromagnetics Research*, Vol. 107, 115–128, 2010.
16. Sun, B.-H., S.-G. Zhou, Y.-F. Wei, and Q.-Z. Liu, "Modified two-element Yagi-Uda antenna with tunable beams," *Progress In Electromagnetics Research*, Vol. 100, 175–187, 2010.
17. Wounchoum, P., D. Worasawate, C. Phongcharoenpanich, and M. Krairiksh, "A switched-beam antenna using circumferential-slots on a concentric sectoral cylindrical cavity excited by coupling slots," *Progress In Electromagnetics Research*, Vol. 120, 127–141, 2011.
18. Hon, T., M.-Z. Song, and Y. Liu, "RF directional modulation technique using a switched antenna array for communication and direction-finding applications," *Progress In Electromagnetics*

Research, Vol. 120, 195–213, 2011.

19. Peng, H.-L., W.-Y. Yin, J.-F. Mao, D. Huo, X. Hang, and L. Zhou, "A compact dual-polarized broadband antenna with hybrid beam-forming capabilities," *Progress In Electromagnetics Research*, Vol. 118, 253–271, 2011.
20. Eom, S. Y., Y.-B. Jung, S. A. Ganin, and A. V. Shishlov, "A cylindrical shaped-reflector antenna with a linear feed array for shaping complex beam patterns," *Progress In Electromagnetics Research*, Vol. 119, 477–495, 2011.
21. Hong, T., M.-Z. Song, and Y. Liu, "RF directional modulation technique using a switched antenna array for physical layer secure communication applications," *Progress In Electromagnetics Research*, Vol. 116, 363–379, 2011.
22. Zaharis, Z. D. and T. V. Yioultsis, "A novel adaptive beamforming technique applied on linear antenna arrays using adaptive mutated boolean PSO," *Progress In Electromagnetics Research*, Vol. 117, 165–179, 2011.
23. Zaharis, Z. D., C. Skeberis, and T. D. Xenos, "Improved antenna array adaptive beamforming with low side lobe level using a novel adaptive invasive weed optimization method," *Progress In Electromagnetics Research*, Vol. 124, 137–150, 2012.
24. Chen, Y., S. Yang, and Z.-P. Nie, "A novel wideband antenna array with tightly coupled octagonal ring elements," *Progress In Electromagnetics Research*, Vol. 124, 55–70, 2012.
25. Li, W.-X., Y.-P. Li, and W.-H. Yu, "On adaptive beamforming for coherent interference suppression via virtual antenna array," *Progress In Electromagnetics Research*, Vol. 125, 165–184, 2012.
26. Jandieri, G. V., A. Ishimaru, V. Jandieri, and N. N. Zhukova, "Depolarization of metric radio signals and the spatial spectrum of scattered radiation by magnetized turbulent plasma slab," *Progress In Electromagnetics Research*, Vol. 112, 63–75, 2011.
27. Wu, X. P., J. M. Shi, S. M. Du, and Y. F. Gao, "Analysis of bi-station scattering characteristics of conductor column covered by time-varying plasma," *Journal of Vacuum Science and Technology*, Vol. 12, 133–141, 2012.
28. Valagiannopoulos, C. A., "Electromagnetic scattering of the field of a metamaterial slab antenna by an arbitrarily positioned cluster of metallic cylinders," *Progress In Electromagnetics Research*, Vol. 114, 51–66, 2011.
29. Xiao, K., F. Zhao, S.-L. Chai, J. J. Mao, and J. L.-W. Li, "Scattering analysis of periodic arrays using combined CBF/P-

FFT method," *Progress In Electromagnetics Research*, Vol. 115, 131–146, 2011.

30. Li, P. and L. Jiang, "The far field transformation for the antenna modeling based on spherical electric field measurements," *Progress In Electromagnetics Research*, Vol. 123, 243–261, 2012.
31. Gomez-Revuelto, I., L. E. Garcia-Castillo, and M. Salazar-Palma, "Goal-oriented self-adaptive HP-strategies for finite element analysis of electromagnetic scattering and radiation problems," *Progress In Electromagnetics Research*, Vol. 125, 459–482, 2012.
32. Pan, X.-M., L. Cai, and X.-Q. Sheng, "An efficient high order multilevel fast multipole algorithm for electromagnetic scattering analysis," *Progress In Electromagnetics Research*, Vol. 126, 85–100, 2012.
33. Zarifi, D., A. Abdolali, M. Soleimani, and V. Nayyeri, "Inhomogeneous planar layered chiral media: Analysis of wave propagation and scattering using Taylor's series expansion," *Progress In Electromagnetics Research*, Vol. 125, 119–135, 2012.
34. Elsherbeni, A. Z. and A. A. Kishk, "Modeling of cylindrical objects by circular dielectric and conducting cylinders," *IEEE Trans. Antennas Propag.*, Vol. 40, 96–99, 1992.
35. Chew, W. C., *Waves and Fields in Inhomogeneous Media*, Van Nostrand Reinhold, New York, 1990.
36. Baizer, Y. P., *Gas Discharge Physics*, Springer-Verlage, Heidelberg, Berlin, 1991.
37. Zhou, T. M., X. Zhou, and W. X. Cai, *Principle and Design of Light Sources*, Fudan University Press, Shanghai, China, 2008.